Rare Metal Materials and Engineering
Volume 48, Issue 10, October 2019
Available online at www.rmme.ac.cn

Science Press

Cite this article as: Rare Metal Materials and Engineering, 2019, 48(10): 3095-3101.

ARTICLE

Microstructural Evolution and Mechanical Properties of Biomedical β-Ti Alloy Prepared by Spark Plasma Sintering Its Prealloyed Powder

Ma Xiqun[1], Niu Hongzhi[2], Su Yongjun[3], Sun Qianqian[2], Zhang Hairui[2], Yu Zhentao[1]

[1] Shaanxi Key Laboratory of Biomedical Metal Materials, Northwest Institute for Nonferrous Metal Research, Xi'an 710016, China; [2] Key Laboratory for Anisotropy and Texture of Materials, Ministry of Education, Northeastern University, Shenyang 110819, China; [3]Lishui University, Lishui 323000, China

Abstract: A biomedical β-Ti alloy Ti-25Nb-3Zr-3Mo-2Sn (wt%) was fabricated via spark plasma sintering (SPS) its prealloyed powder. The prealloyed powder was produced by plasma rotating electrode process. The results show that most powder particles have a microstructure composed of β-phase predominated dendrites, while a tiny fraction of the powder particles have a single crystal microstructure. SPS conducted under 1000 °C, 5 min and 50 MPa condition can completely densify this β-Ti alloy powder and eliminate its prior dendritic segregation. After solution treatment, the consolidated alloy has a microstructure consisting of $\alpha''+\beta$ phase, and exhibits a good tensile strength of 815 MPa and an optimal elongation of 14%, as well as a low elastic modulus of only 62 GPa. Aging at 500 °C brings a large number of nano-sized α needles, which render this alloy excellent tensile strength up to 1015 MPa along with elongation and elastic modulus both acceptable. However, excessively low aging temperature should be avoided, due to the sharp embrittlement induced by nano-scale ω-phase precipitates.

Key words: β-Ti alloy; prealloyed powder; spark plasma sintering; microstructure; mechanical properties

Titanium alloys are widely used as biomedical implants due to their outstanding advantages such as superior specific strength, excellent corrosion resistance, biocompatibility etc[1-3]. Meanwhile, β-type titanium alloys with non-toxic alloying elements such as Nb, Mo, Ta, Zr, Sn are developed to replace the generally used CP-Ti and Ti-6Al-4V [4,5]. Nb, Mo, Ta are added as β-phase stabilizers, in order to promote biocompatibility and biomechanical compatibility, whereas Zr and Sn are neutral elements in terms of phase stabilization. Moreover, such β-Ti alloys are most satisfying to make the elastic modulus of implants closer to that of human hard tissues [6,7]. This is rather favorable for relieving so-called "stress-shielding" effect in Ti alloy implants.

Ti-25Nb-3Mo-3Zr-2Sn (hereinafter referred to as TLM) is a typical biomedical near β-Ti alloy developed by Northwest Institute for Nonferrous Metal Research (NIN), based on *d*-electron alloy design theory. This alloy is normally produced by ingot metallurgy route, and shows an excellent combination of high tensile yield strength, superior elongation and a favorable low elastic modulus [7-9]. The mechanical properties of TLM alloy greatly depend on various phase transformation products from the β parent phase, such as hexagonal α phase, metastable hexagonal ω (always nano-sized), orthorhombic α'' martensites[5,9-11], which is similar to other β-Ti alloys. It has been generally accepted that, in β-Ti alloys, the elastic modulus and hardness arranged in descending order are: $\omega>\alpha>\alpha''>\beta$ [11,21].

Powder metallurgy (PM) is a desirable low-cost means to producing titanium alloys and their complex components via near-net forming. Meanwhile, PM process avoids microstructural heterogeneity and composition segregation problems

Received date: October 09, 2018
Foundation item: National Natural Science Foundation of China (51801162); Fundamental Research Funds for the Central Universities (02080022117003)
Corresponding author: Yu Zhentao, Ph. D., Professor, Shaanxi Key Laboratory of Biomedical Metal Materials, Northwest Institute for Nonferrous Metal Research, Xi'an 710016, P. R. China, Tel: 0086-29-86222297, E-mail: yzt@c-nin.com

which are always caused by ingot metallurgy route. In particular, considering the large difference in melting point, density and diffusion coefficient of Ti, Nb, Mo, Ta, Zr, Al, Sn, etc in Ti-based alloys[12-14], the superiority of PM process is more remarkable. Compared with blending elemental method [15], prealloyed powder process is more feasible to fabricate high relative density and high-purity titanium alloys with accurate chemical composition. Spark plasma sintering (SPS) is a novel rapid powder consolidation technique used in preparing high relative density and fine-grained materials from titanium prealloyed powder[12,13]. Plastic deformation of powder particles is considered to be the main mechanism responsible for SPS densification. In particular, compared with hot press sintering and pressureless sintering, the joule heat effect generated during SPS is very beneficial to solute homogenization and dissolution of oxide layers on the surfaces of powder particles.

By now, research on metastable β-Ti alloy via SPS of prealloyed powder has not yet been conducted. In this study, SPS was adopted to prepare a biomedical β-Ti alloy TLM using its prealloyed powder. The SPS densification process, microstructural evolution from original powder to post-processing heat treatments, microstructure characteristics and corresponding mechanical properties were investigated systematically. Besides, a hot-rolled bar of this alloy via ingot metallurgy route was chosen to compare microstructures and properties. The ultimate aim of the study is to explore an alternative way for producing high-quality biomedical β-Ti alloys.

1 Experiment

Prealloyed powders of TLM alloy Ti-25Nb-3Zr-3Mo-2Sn (wt%) were produced by plasma rotating electrode process (PREP). Cast ingots with diameter of 160 mm were prepared by vacuum arc remelting (VAR) for two times, and then processed into cylindrical bars with diameter of 75 mm for powder production. The PREP powder was screened to obtain −100 mesh powder for SPS, and the particle sizes of the sieved powder are D 10: 80 μm, D 50: 100 μm and D 90: 130 μm. The chemical composition of the powder was measured to be Ti-24.92Nb-3.12Zr-3.15Mo-1.95Sn (wt%) by ICP-OES method (inductively coupled plasma optical emission spectrometry), and the oxygen content is determined to be 0.01% by Brook oxygen-nitrogen-hydrogen (ONH) analyzer.

All SPS experiments were performed on a FCT-HPD 25/4-SD SPS system (FCT system GmbH) at temperatures of 950, 1000 and 1050 °C and a constant pressure of 50 MPa for a holding time of 5 min or 10 min. After SPS, the samples were quickly cooled in the die by argon flow, and several alloy disks with dimensions of Φ52 mm×9 mm were obtained. The alloy sample subjected to SPS at 1000 °C for 10 min had an oxygen content of 0.18% and exhibited a β-transition temperature (T_β) close to 730 °C by DIL805A/D thermal expansion deformation phase change instrument. In contrast, the oxygen content of a TLM hot-rolled bar via ingot metallurgy used for comparison was only 0.11 μL/L.

The microstructures of the samples were characterized by X-ray diffraction (XRD), optical microscopy (OM), scanning electron microscopy (SEM) and transmission electron microscopy (TEM) techniques. Electron probe micro-analyzer (EPMA) was used to measure the elemental distribution. XRD measurements were conducted on a SmartLab X-ray diffractometer with Cu Kα radiation at a scan rate of 3°/min. The optical microscopy observation was conducted using a Zeiss microscope. For high-magnification microstructure observation, field emission SEM (JSM-6700) and a 200 kV TEM (JEOL JEM-200CX) were adopted. TEM foils were prepared by standard mechanical polishing and twin-jet electropolishing using a solution of 6% perchloric acid+34% butanol+60% methanol at −20 °C and 25 V.

In order to adjust microstructures of the sintered samples, solution and aging treatments were conducted for certain fully densified samples in a program-controlled muffle furnace. Solution was carried out at 800 °C (i.e. 70 °C higher than T_β) for 10 min to relieve stress concentration and to dissolve all the alloying elements in single β phase. Further, aging treatment was performed at lower temperatures within $\alpha+\beta$ phase to precipitate different strengthening phases. The tensile tests were performed on an Instron 5500R machine at a cross-head speed of 0.5 mm/min at room temperature. Rounded bar- shaped tensile test specimens with gauge sections of 3 mm in diameter and 20 mm in length were used. To determine the accurate Young's modulus values, the impulse excitation technique (IET) was adopted.

2 Results and Discussion

2.1 Microstructural characteristics of the PREP prealloyed powder

Fig.1 presents the rapidly-solidified microstructures of TLM prealloyed powder produced by PREP. As shown, most powder particles exhibit dendritic microstructures and surface morphology (Fig.1a and 1c), while a tiny fraction of the powder particles display a single phase microstructure with featureless smooth surfaces (Fig.1b and 1d). This is mainly related to size of liquid droplet formed during PREP. The smaller the liquid droplet size, the faster the solidification speed. Thus solid-liquid interface can move forward quickly, and almost no time is left for alloying element diffusion and redistribution within the micro areas near solid-liquid interface. This induces featureless single crystal powder particles. Meanwhile, it is found that the dendritic microstructure is underdeveloped and the secondary dendrite arms are extremely small. Such rapidly-solidified microstructure of β-Ti alloy is also found in PREP prealloyed powders of Ti2AlNb alloy with high β-stabilizer content of 42.5 wt% Nb[12].

Fig.2 displays the elements distribution within a powder particle with dendritic microstructure. The refractory elements Nb and Mo have the same distribution features. They prefer to

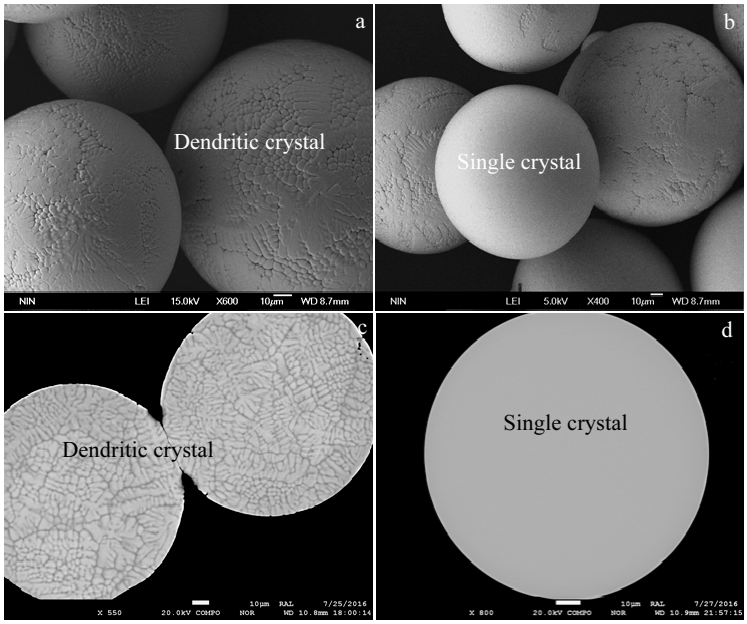

Fig.1 Morphologies and microstructures of rapidly-solidified Ti-25Nb-3Zr-3Mo-2Sn prealloyed powders: (a) dendritic crystal, (b) dendritic and single crystal, (c) dendritic crystal, and (d) single crystal inside powder particles

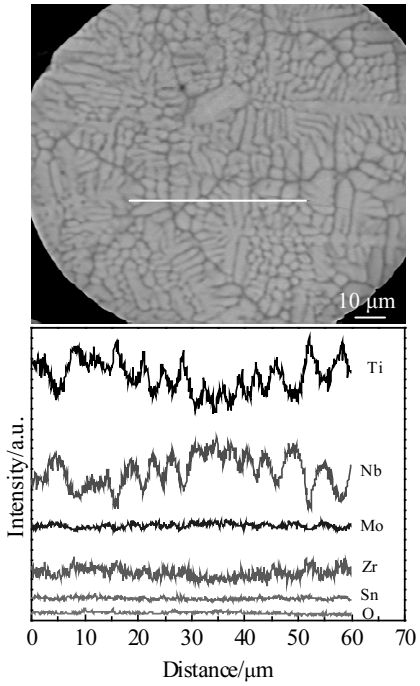

Fig.2 Elemental distribution within a dendritic powder particle (EPMA)

exist inside dendrites. Conversely, others, including Ti, Zr, Sn and O tend to exist in interdendritic areas and at boundaries of second dendritic arms, where they are relatively more diffusible than Nb and Mo. During rapid solidification, these solute atoms are easier to be ejected from crystal growth areas and are redistributed.

As shown in Fig.3a, the diffraction peaks of bcc β and orthorhombic α'' phases are both visible on the XRD patterns of the powder. This indicates that α'' martensites form during PREP. Through acid etching, fine globular α'' martensites can be revealed, as shown in Fig.3b. These α" martensitic globules cannot be recognized by SEM in BSE mode, as shown in Fig.1c and 1d, mainly because they have almost the same element contents as the β matrix. These α'' globules in the TLM prealloyed powder particles are formed by rapid cooling of small liquid droplets during PREP. On the other hand, TLM is a near β-Ti alloy having a relatively low molybdenum equivalent [Mo] value close to 10, which is insufficient to stabilize the β parent phase during rapid cooling, leading to the formation of α'' martensites.

2.2 SPS densification process and sintered microstructures

Fig.4 presents the densification process of SPS and the microstructural evolution. SPS under a condition of 950 °C, 50 MPa and 5 min only brings a porous microstructure, shown in Fig.4a. Cavities among prior powder particles can be observed clearly, though powder particles are contacted locally and sintering necks have formed. Besides, original dendritic segregation remains inside some powder particles. This indicates that SPS temperature of 950 °C is neither high enough for full densification via severe plastic deformation of powder particles nor sufficient for thorough diffusion of alloying elements. After increasing the sintering temperature to 1000 °C, a fully dense microstructure is formed, without micro pores, as shown in Fig.4b.

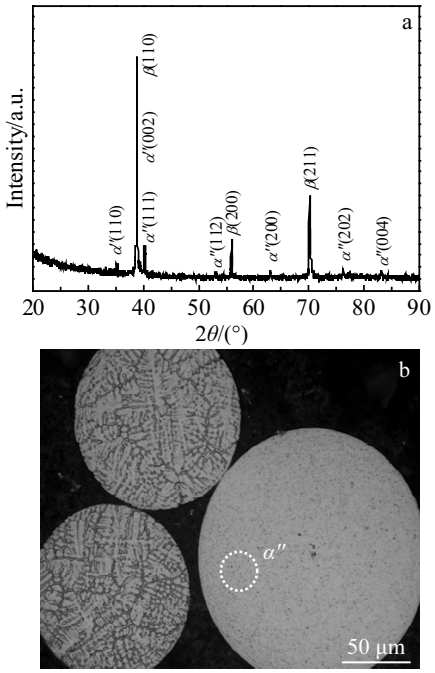

Fig.3 XRD pattern (a) and OM image (b) of prealloyed powders (etched by acid)

Considering that very small pores may survive and in order to guarantee a sufficient metallurgical bonding among the powder particles, a longer SPS duration of 10 min at 1000 °C and a higher SPS temperature of 1050 °C were used, as shown in Fig.4c and 4d, respectively. They both give rise to fully dense β-phase predominated microstructures mainly decorated by α'' globules at grain boundaries. The densification behavior of current TLM alloy powder during SPS is almost the same as that found in a Ti-22Al-25Nb (at%) prealloyed powder[12].

2.3 Effect of heat treatments on microstructural evolution

Fig.5 displays phase composition, and Fig.6 shows microstructures of the fully dense sintered TLM alloy under various heat treatment conditions. After SPS at 950 °C for 10 min, the microstructure of the as-sintered sample consists of β and martensitic α'' phases. The martensitic α'' phase is also found in solution treated state. As observed in Fig.6a and 6b, the solution treated microstructure is dominated by β phase with an average grain size of about 60 μm. Fine α'' phase globules are also present in the microstructure, which are mainly located at grain boundaries. For near β-Ti alloys, because of the thermodynamic instability of β parent phase, α'' martensites are readily induced via $\beta \rightarrow \alpha''$ transformation by stress[5,9,16,17] or quenching at temperatures above β-transition temperature[7,18].

Further aging treatment at 500 °C causes dissolution of the α'' globules, and a large number of nano-sized α needles are formed in the matrix of β-phase. Some needles near the grain boundaries grow longer, as shown in Fig.6d. However, aging at an excessively low temperature of 380 °C only brings hexagonal ω phase. These ω phase precipitates are densely distributed and also extremely fine, as shown in Fig.6e and 6f.

The detailed morphologies of α and ω phase precipitates are revealed by TEM observations. As shown in Fig.7a, nano-sized acicular α precipitates, thinner than 40 nm and shorter than 400 nm, can be clearly seen within the matrix of β phase. In comparison, the ω phase precipitates are also nano-sized but have oval shapes (Fig.7b). Such ω phase is generally formed by

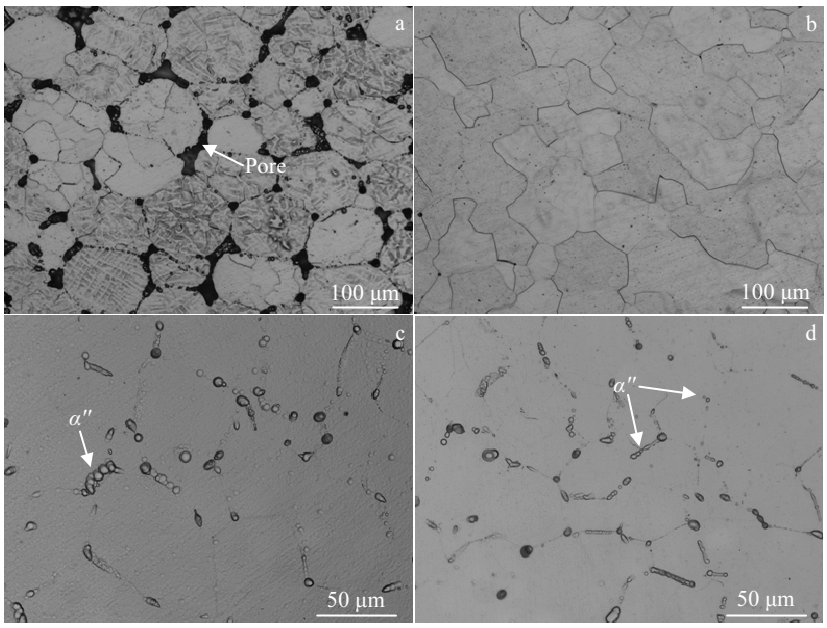

Fig.4 As-sintered microstructures of the prealloyed powders by SPS under different conditions: (a) 950 °C-50 MPa-5 min; (b) 1000 °C-50 MPa-5 min; (c) 1000 °C-50 MPa-10 min; (d) 1050 °C-50 MPa-10 min

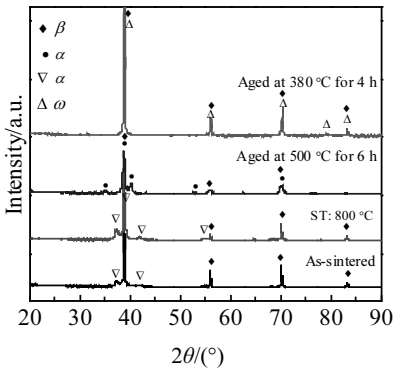

Fig.5 XRD patterns of TLM alloy in different states

quenching from β-phase field area (isothermal ω phase)[19], by aging/annealing (isothermal ω phase)[7,9,19] and deformation of the low-stability β phase [20]. And the orientation relationship between ω phase and β phase is determined as $(0001)_\omega//(1\bar{1}1)_\beta$ and $(1\bar{1}00)_\omega//(21\bar{1})_\beta$, $[11\bar{2}0]_\omega//[011]_\beta$ [9].

2.4 Evaluation of mechanical properties

Fig.8 lists the room-temperature (RT) tensile properties of the SPS TLM alloy at various heat-treatment states. Solution treatment at 800 °C (ST-800 °C) produces the lowest yield strength (YS) of only 535 MPa and ultimate tensile strength (UTS) of 815 MPa, but the best elongation up to 14% and the most favorable elastic modulus of 62 GPa. After aging at 500 °C (STA-500 °C-6 h), the YS and UTS values increase to 950 and 1015 MPa, respectively, while elongation drops down to 8.5% and modulus value reaches 78 GPa. Aging at a much lower temperature of 380 °C (STA-380 °C-4 h) remarkably increases the strength and elastic modulus, but sharply deterio-

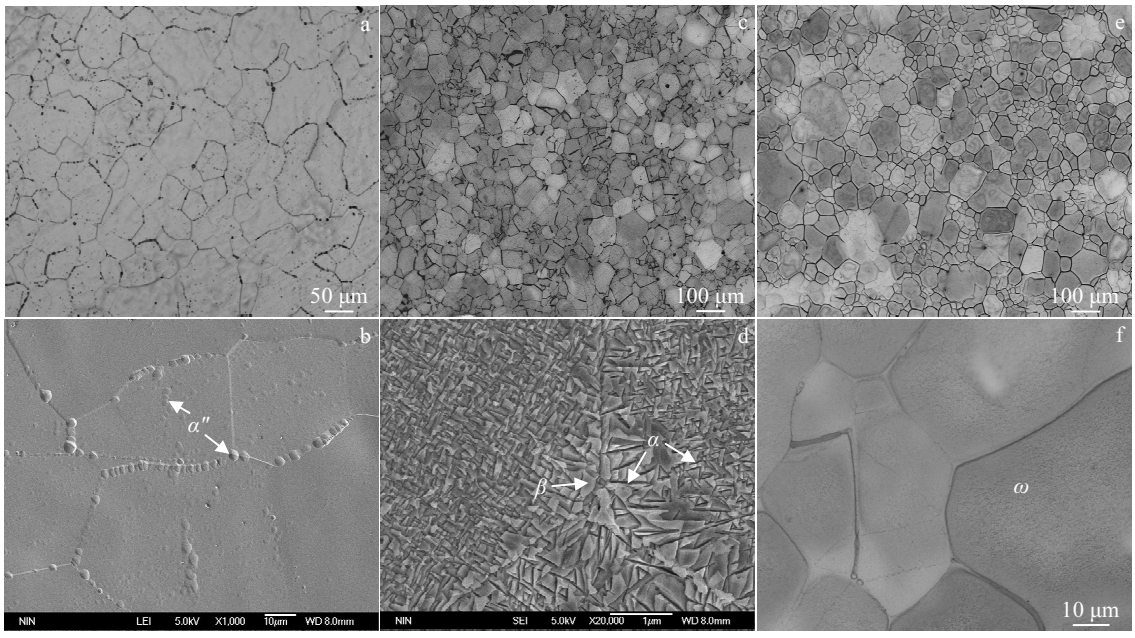

Fig.6 Microstructures of sintered alloy undergone different heat treatments: (a, b) solution treatment at 800 °C, (c, d) aging at 500 °C for 6 h, and (e, f) aging at 380 °C for 4 h

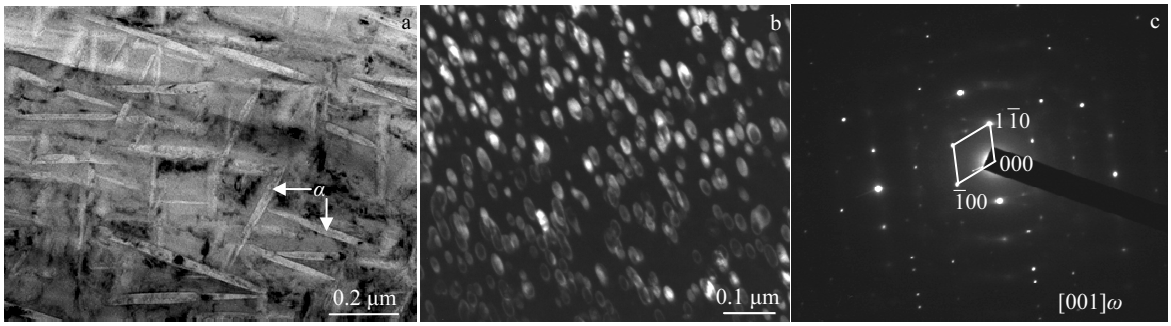

Fig.7 TEM images of the precipitated phases: (a) acicular α phases, taken in bright-field mode, (b) nano-sized ω phases, in dark-field mode, and (c) corresponding selected-area electron diffraction pattern taken along zone axis [001] of ω phase

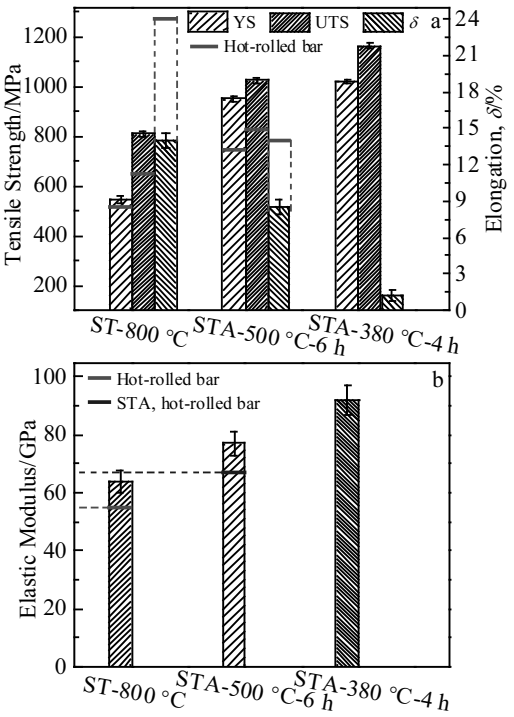

Fig.8 Mechanical properties of the present SPS TLM alloy: (a) tensile properties and (b) elastic modulus (corresponding properties of a hot-rolled bar of the same alloy produced by ingot metallurgy route were marked by red color for comparison)

rates elongation. It has been reached a consensus that in metastable β-Ti alloys, ω phase is brittle and provides the highest Young's modulus, but β phase offers the lowest Young's modulus[11,21]. Therefore, aging temperature should be high enough to prevent precipitation of brittle ω phase.

For comparison, mechanical properties of a TLM alloy hot-rolled bar produced by ingot metallurgy and final hot rolling were also investigated. As marked in Fig.8, in solution treatment state or 500 °C aging state, the hot-rolled alloy always exhibits much lower strength, more desirable elastic modulus along with remarkably better ductility. In particular, under solution treated condition, hot-rolled bar presents a satisfying modulus value as low as 55 GPa and a superior elongation up to 24%. After aging treatment, its elongation decreases sharply to 14% while modulus value increases rapidly to 67 GPa. However, the yield strength of this hot rolled bar is 130 MPa, lower than that of the SPS TLM alloy.

3 Discussion

For β-type Ti alloy, it is reported that its mechanical properties are closely depended on phase transformation products of metastable β parent phase, such as hexagonal ω, orthorhombic α" and hexagonal α phases[5-9]. In this study, aging at 500 °C induces precipitation of special nano-sized α needles in a massive amount, resulting in a high YS of 950 MPa and a moderate Young's modulus of 78 GPa along with an acceptable elongation of 8.5%. Compared with the as-aged microstructures of TLM alloy produced by ingot metallurgy, such as cold rolled sheet in Ref. [9] and hot-rolled bar 500 °C aged in Fig.9, the morphologies of α precipitates in the current SPS alloy are much special, especially in thickness and length values of α needles. This can be verified directly in Fig.9, where α phase needles spread through individual β grains, indicating that the maximum length of these α needles are almost equal to that of individual β grain.

In addition, the density of needle-like α precipitates within β grains of SPS TLM alloy is apparently enhanced, which may be directly induced by a relatively higher oxygen content of 0.18%. Because, as is well known, oxygen is a strong α-phase stabilizer in titanium alloy, which promotes intensive and uniform nucleation of α phase during isothermal aging. Thus, high contents of nano-sized α needles and corresponding α/β interfaces can be produced. This is the two key strengthening factors for β-Ti alloys, essentially due to strong dislocation blocking effect. Meanwhile, proper increase in oxygen concentration can play an important role in hardening as well[14,20,22]. Finally, the high density of nano-sized α needles together with a properly high oxygen concentration results in a superior tensile strength in current SPS TLM alloy.

As to the resultant elastic modulus of this as-aged SPS TLM alloy, it is about 10 GPa higher than that of hot-rolled TLM alloy produced by ingot metallurgy. However, it is still

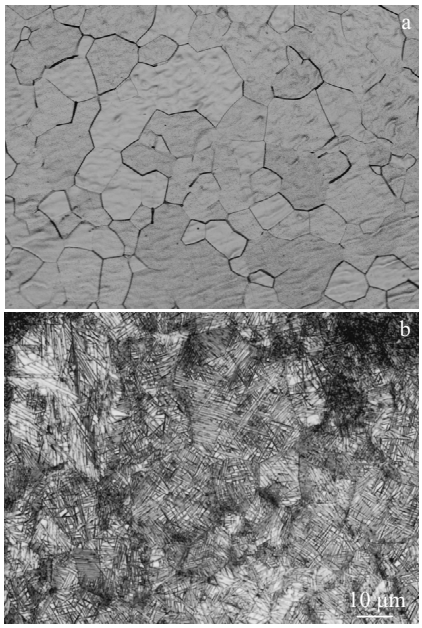

Fig.9 Microstructures of a hot-rolled TLM alloy bar produced by ingot metallurgy: (a) solution treated under 800 °C-1 h-WQ and (b) aged under 500 °C-6 h-FC

significantly lower compared with almost 110 GPa of the commonly used Ti-6Al-4V titanium alloy[1,11]. Meanwhile, the present SPS TLM alloy exhibits much higher strength than Ti-6Al-4V (~950 MPa) and contains no toxic elements. In short, this SPS TLM alloy is feasible for biomedical applications, especially as a load-bearing implant.

4 Conclusions

1) SPS is entirely feasible for fabricating a fully dense biomedical β-Ti alloy from its prealloyed powder.

2) SPS under condition of 1000 °C-50 MPa-10 min is proposed to transform the prealloyed powder of dendritic and single crystal structures into a fully dense β-predominated microstructure.

3) SPS accompanied with microstructural adjustments is adopted to produce a high-quality biomedical near β-Ti alloy. Solution and aging treatment can provide superior tensile yield strength up to 950 MPa and low modulus of 78 GPa, as well as an acceptable elongation of 8.5%.

4) High number density of nano-sized α needles along with a properly high oxygen content play a great role in strengthening current SPS TLM alloy.

References

1 Geetha M, Singh A K, Asokamani R *et al*. *Progress in Materials Science*[J], 2009, 54: 397

2 Rack H J, Qazi J I. *Materials Science and Engineering C*[J], 2006, 26(8): 1269

3 Long M, Rack H J. *Biomaterials*[J], 1998,19(18): 1621

4 Stráský J, Harcuba P, Václavová K *et al*. *Journal of the Mechanical Behavior of Biomedical Materials*[J], 2017, 71: 329

5 Wang L Q, Lu W J, Qin J N *et al*. *Materials & Design*[J], 2009, 30(9): 3873

6 Chen J, Ma F C, Liu P *et al*. *Vacuum*[J], 2017, 146: 164

7 Yu Z T, Zhou L. *Materials Science and Engineering A*[J], 2006, 438-440: 391

8 Kent D, Wang G, Yu Z T *et al*. *Journal of the Mechanical Behavior of Biomedical Materials*[J], 2011, 4(3): 405

9 Ma X Q, Niu H Z, Yu Z T *et al*. *Rare Metals*[J], 2018, 37(10): 846

10 Hao Y L, Yang R, Niinomi M *et al*. *Metallurgical and Materials Transactions A*[J], 2003, 34(4): 1007

11 Fan Z. *Scripta Metallurgica et Materialia*[J], 1993, 29: 1427

12 Niu H Z, Chen Y F, Zhang D L *et al*. *Materials & Design*[J], 2016, 89: 823

13 Niu H Z, Su Y J, Zhang Y S *et al*. *Intermetallics*[J], 2015, 66: 96

14 Wen M, Wen C, Hodgson P *et al*. *Materials and Design*[J], 2014, 56: 629

15 Nazari K A, Nouri A, Hilditch T. *Materials and Design*[J], 2015, 88: 1164

16 Appolaire B, Settefrati A, Aeby-Gautier E. *Materials Today Proceedings*[J], 2015, 2(S2): 589

17 Yao T T, Du K, Hao Y L *et al*. *Materials Letters*[J], 2016, 182: 281

18 Mantani Y, Tajima M. *Materials Science and Engineering A*[J], 2006, 438-440: 315

19 Nejezchlebova J, Janovska M, Seiner H *et al*. *Acta Materialia*[J], 2016, 110: 185

20 Liu H H, Niinomi M, kiNakai M *et al*. *Acta Materialia*[J], 2016, 106: 162

21 Collings E W. *Physical Metallurgy of Titanium Alloys*[M]. Ohio: ASM Series in Metal Processing, 1984

22 Wei Q Q, Wang L Q, Fu Y F *et al*. *Materials & Design*[J], 2011, 32(5): 2934

放电等离子烧结预合金粉末法制备生物医用近β钛合金的组织演变和力学性能

麻西群[1]，牛红志[2]，苏勇君[3]，孙倩倩[2]，张海瑞[2]，于振涛[1]

(1. 西北有色金属研究院 陕西医用金属材料重点实验室，陕西 西安 710016)

(2. 东北大学 材料织构与各向异性教育部重点实验室，辽宁 沈阳 110819)

(3. 丽水学院，浙江 丽水 323000)

摘 要：利用放电等离子烧结(SPS)预合金粉末的方法，成功制备出生物医用的近β钛合金 Ti-25Nb-3Zr-3Mo-2Sn (质量分数，%)。近β钛合金的预合金粉末利用等离子旋转电极法制备，粉末的凝固组织主要是由β相主导的不发达的树枝晶组成，同时存在少量的β相单晶组织粉末球。1000 ℃-5 min-50 MPa 条件下的 SPS 可以完全致密化近β钛合金的预合金粉末，并且消除原始的凝固偏析结构。β单相区固溶处理后，合金组织由β相和α''相组成，合金的抗拉伸强度达到 815 MPa，延伸率达到 14%，同时具备 62 GPa 较低的弹性模量。进一步 500 ℃时效处理，合金组织中产生大量的纳米针状σ相，使得合金的抗拉伸强度达到 1015 MPa，同时具备较好的延伸率和中等的弹性模量。然而，应当避免过低的时效处理温度，防止脆性ω相的析出。

关键词：近β钛合金；预合金粉末；放电等离子烧结；显微组织；力学性能

作者简介：麻西群，女，1981 年生，硕士，高级工程师，西北有色金属研究院陕西医用金属材料重点实验室，陕西 西安 710016，电话：029-86222297，E-mail: maxiqun23@126.com